# Long records of weather at Jungfraujoch as climate input

C. Appenzeller et al.

Federal Office of Meteorology and Climatology MeteoSwiss

At the Jungfraujoch the Federal Office of Meteorology and Climatology MeteoSwiss operates the highest permanently manned meteorological station in Europe. Measurements have been carried out since 1922 when the access by railroad was completed and the Jungfraujoch commission was founded. Today, long term data series of stations on such altitudes are of great value to address Alpine specific questions of the current global change debate. In this talk we will compare Jungfraujoch measurements with those of other stations and explore the different impact of past and future climate change at high and low altitudes.

# Short-term acclimatization to high altitude in children compared to adults

S. Kriemler

Institute for Sports and Sport Sciences, University of Basel, Switzerland

Introduction: There is very little known about the short-term adaptation of children to high altitude, despite the fact that more and more children travel to those altitudes for recreational reasons such as skiing or trekking. The general objectives of this study were therefore to determine short-term (3-day exposure) altitude-related (3450m above sea level) changes of pulmonary, cardiovascular functions at rest, during exercise and sleep, and the tolerance of altitude and occurrence of AMS in prepubescent children. Specifically, we compared function between low altitude (LA) and day 1-3 at high altitude (HA) among the healthy, prepubertal 9-12-year-old children, and in comparison to their fathers. We were also interested in possible genetic similarities between fathers and children.

Measurements: The following measurements were taken at LA and on day 1, 2 and/or 3 of HA: clinical exam, score of acute mountain sickness by questionnaire, resting pulmonary function, echocardiography, hypoxic ventilatory response, a maximal aerobic exercise test on a stationary bike, fluid and energy balance, and respiratory plethysmography.

Results: The cumulative incidence of acute mountain sickness (AMS) was similar in children and adults when measured with the Lake Louise- or the AMS-C-Score (Figure 1). However, a tendency that children became more sick was apparent considering the AMS-C-Score with 10 sick children vs. 6 sick adults (p=0.1), but due to the small study sample significance was missed. All children and their fathers were sick within 30 hours of altitude exposure, on day 3 of HA all participants were healthy again. These results have to be interpreted with caution, since adult questionnaires were used in a population of children who might have problems to read and interpret the questionnaires as well as to give appropriate responses.

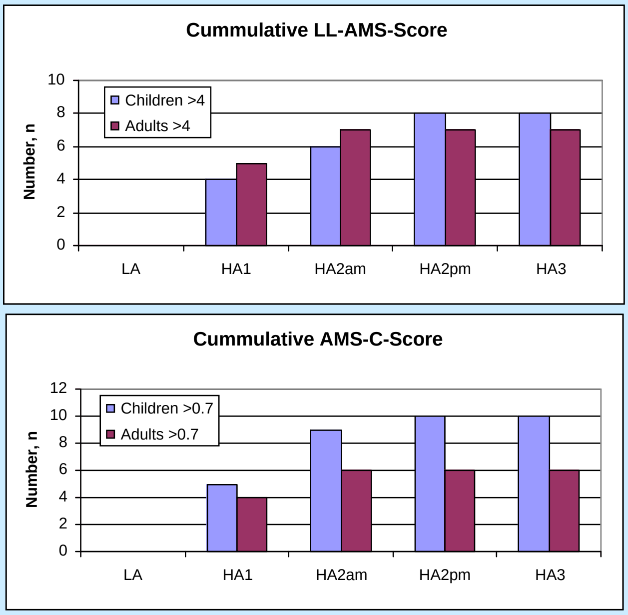


Figure 1: Cumulative AMS-C-Score and LL-AMS Score in children and adults, respectively

Maximal aerobic exercise performance at LA was similar in children and adults, respectively, when corrected per bodyweight. Both reduced their $VO_2$max similarly by about 20% on day 1 and 3 of HA. But the heart rate behaved differently. While it stayed at equal levels at LA and HA in children, it decreased significantly from LA to HA in adults on both days at HA. It seems, therefore, that the cardiovascular response to HA is different in children and adults.

Isocapnic hypoxic ventilatory response (HVR), a measure of respiratory responsiveness to hypoxia, was higher in children than in adults irrespective of altitude (Figure 2). Both groups increased their HVR with HA, but only adults showed a significant increase of HVR on day2. Neither HVR at LA nor at HA was correlated with AMS in both groups. Whether the extent of the drive at LA, or the extent of increase at HA is important for the protection against AMS, is still controversial even among the adult population.

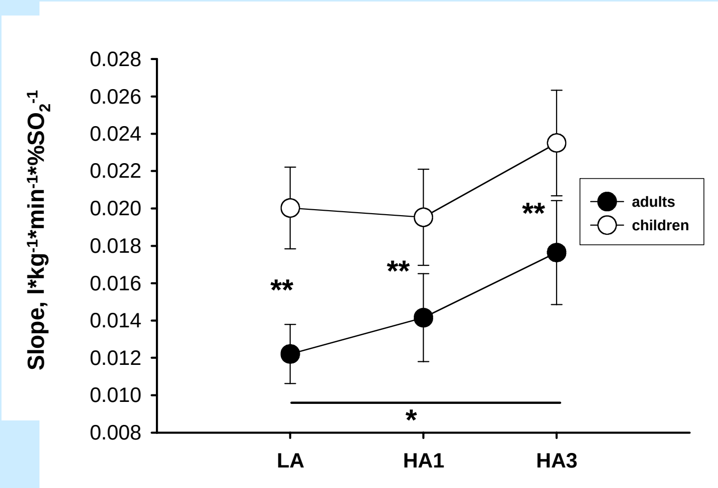


Figure 2: Hypoxic ventilatory response, expressed as $\Delta VE*kg^{-1}*min^{-1}/\Delta SO_2$ in children and adults at LA and day 1 and 2 of HA.

With HA, pulmonary artery pressure increased significantly in both groups, but increased significantly more in children than in adults (Figure 3). This could be one important factor why children might become sicker at HA than adults. A postulated mechanism why a high pulmonary artery pressure might lead to more AMS is an inhomogeneous vasoconstriction in the pulmonary arteries leading to a diffusion limitation of oxygen into the blood.

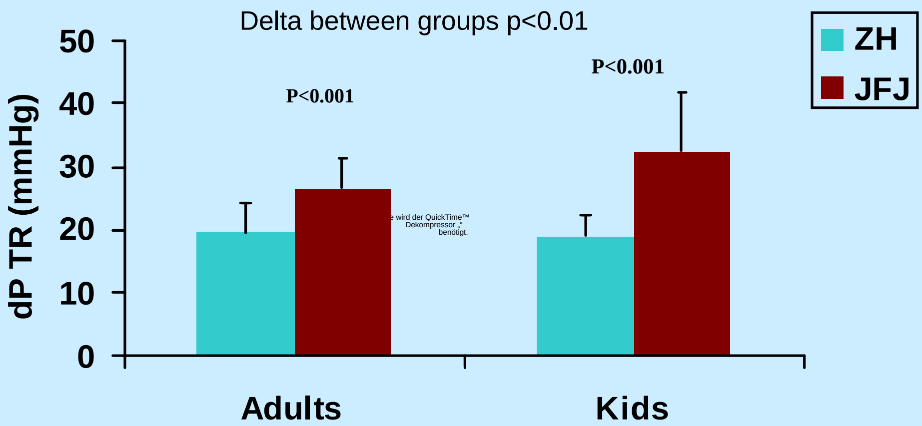


Figure 3: Pressure gradient over the tricuspid valve which then is converted to pulmonary artery pressure (PAP).

Conclusion: Despite several physiological differences in short-term adaptation to HA, in general, children behave similarly than adults.

Acknowledgment**:** We thank all the children and adults who took part in this demanding but also challenging project. We also thank the foundation HFSJG, with a special thank to Prof. E. Flückiger, L. Wilson, J. and M. Fischer, G. and K. Hemund for the excellent support. And finally, we thank the Federal council of Sports in Magglingen, Switzerland for the support of the study.

(1.8)
## Atmospheric Aerosol and Solar Activity

I. A. Mironova and D.I. Ponyavin

Institute of Physics, St.Petersburg State University,
St.Petersburg, Russia 198504

According to present-day ideas, solar activity affects the state of the low atmosphere by means of modulation of the cosmic ray flux intensity, which can change cloudiness, traces gases and aerosol layer. Thereby an aerosol can be one of the important parameters of the atmosphere in a mechanism of solar - terrestrial relationship. The aim of this work is to study the variations of the aerosol optical parameters depending on a change in solar activity. Data on the aerosol optical thickness and aerosol backscatter vertical profiles, which characterize a vertical change in aerosol optical properties, were selected for analysis. There are also studied the long- and short- term aerosol variations, volcanic eruptions, geomagnetic and solar activities.

The long-period variations in the multispectral aerosol optical thickness in the period from 1979 to 1994 are analyzed depending on the volcanic eruptions and solar cycle. It has been indicated that two maximums at an interval of 11 years, along with the seasonal variations in the aerosol optical thickness, are clearly defined during this period. Strong volcanic eruptions occurred a year before the maximums of the aerosol optical thickness. In the given case, this supposedly means that ejections after two strong volcanic eruptions, rather than solar activity maximums, could be responsible for the two large maximums in this time interval.

The short-period variations in aerosol backscatter are analyzed depending on the solar proton events. The results obtained indicate that a rather thick aerosol layer (instead of a thin layer) is formed at an altitude of about 10 km in the atmosphere after precipitation of protons with energies higher than 100 MeV. The backscatter coefficient increases by an order of magnitude as compared to its value on a quiet day, when precipitation of energetic particles is not observed. Several days later, the situation becomes stable and the backscatter coefficient decreases. It is finally concluded that solar activity can be an additional factor responsible for aerosol optical properties.

(3.9)
**Kr-85 measured at Jungfraujoch and elsewhere:**
**A versatile global tracer**

R. Purtschert[1], H. Sartorius[2] H. H. Loosli[1], R. Riedmann[1], C. Schlosser[2], S. Schmid[2]

1 University of Bern, Switzerland
2 Bundesamt für Strahlenschutz, Freiburg i. Br., Germany

Kr-85 is a radioactive noble gas with a half-life of 10.76 years. Since more than 15 years the tropospheric Kr-85 activity has been continuously monitored at Jungfraujoch (JFJ). This sampling location is unique in Europe because the high altitude is ideal for the determination of the tropospheric background activity of Kr-85. At lower elevations in Europe spikes of higher activities are frequently observed. This $^{85}Kr$ enriched air masses originate from reprocessing facilities for nuclear fuel. In the paper, its is emphasized how the Kr-85 data from JFJ and elsewhere can be used to:

- monitor the reprocessing activities world wide.
- validate and calibrate global and local circulation models.
- determine the residence time of groundwater in the subsurface.

## A versatile seeing monitor for smaller observatories

François Wildi, Benjamin Girardet

HEIG-VD, West Switzerland University of Applied Sciences, CH-1400 Yverdon

Introduction

Traditionally, the evaluation of the seeing at an astronomical site is done using the long exposure Point Spread Function (PSF) with is largely sufficient for classic instruments. We believe that the emergence of large stoke medium order deformable mirrors [1] offers an opportunity to develop low-cost line-of-sight Adaptive Optics (AO) systems for small telescopes. These systems can improve both resolution to the diffraction limit in the visible and throughput of spectrographs.

However, it is crucial to know a number of atmospheric parameters and in particular the spatio-temporal behaviors of the turbulence when dimensioning the AO system and predicting the improvement that can be brought with real-time correction. This is why we have developed a site seeing monitor using the Differential Image Motion Monitor principle. We intend to take it to different observatories that do not have their own instrument for measurement campaigns. Currently, the seeing monitor is capable of delivering an instantaneous value of the Fried parameter r0 every 10s

Principle of the measurement

In first order the atmospheric turbulence will add a time-varying random phase fluctuation to the initially plane wavefront coming from a point-source at infinity. With the hypothesis of Kolmogorov turbulence, one can demonstrate [3] that the covariance of the angle of arrival of the wavefront after atmospheric distortion is:

$$B_\alpha(\xi,0) = 0.097\left(\frac{\lambda}{r_0}\right)^{5/3}\left(\frac{\lambda}{\xi}\right)^{1/3} \text{ and } B_\alpha(0,\eta) = 0.145\left(\frac{\lambda}{r_0}\right)^{5/3}\left(\frac{\lambda}{\eta}\right)^{1/3}$$

It is therefore possible to link the covariance of the angle of arrival of 2 images through two distinct apertures to the Fried parameter r0 that characterizes the coherence length of the atmosphere.

The instrumental principle is to image a source through two sub-apertures of a small telescope and separate them somehow in the image plane. A set of short exposure images is taken and the differential position of the images formed by the sub-wavefronts is computed for each of them. Computing the variance of this position yields the Fried parameter through the equation above.

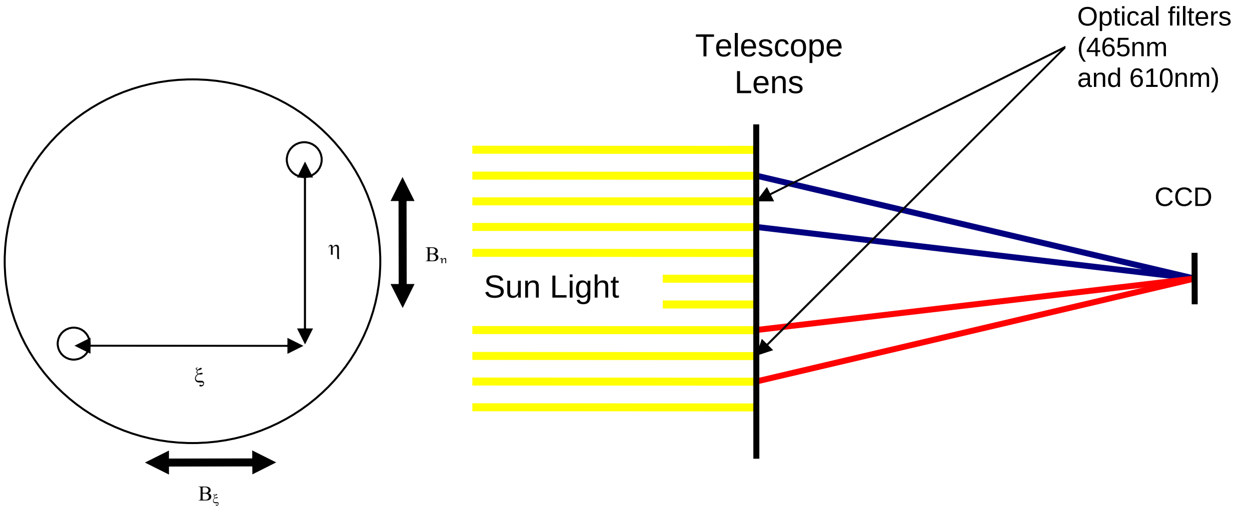


Implementation
The setting of the DIMM is different for night and day-time. In the first case, there is a lot of punctual objects with limited intensity and for the second case there is only one extended-field object. In both cases, the entrance pupil is devided in 2 (or 3) sub-pupils situated at the periphery of the original 300mm pupil. The images given by the sub-pupils must be separated before processing.

During night-time, as the image of a star is a spot, the beam of one sub-pupil is tilted with a prism to shift its image on the camera. The centroïd positions can then be directly extracted from the images and thus the differential shift between the spots.

For day-time the mask is featuring two small pupils with 10nm FWHM filters (465nm and 610nm) that will produce one image on the blue pixels, and one image on the red pixels of a color camera. This particular setting allows us to get distincts collocated images from the two sub-pupils by interpolating between the color filters built atop the pixels of the camera. To extract the image motion, we use the image of the Sun's limb and take the maximum of the cross-correlation function between two images from the same sub-aperture at time k and k+1 give us the shift value between the two images. The difference between the blue-shift and red-shift is the differential motion between the sub-pupils.

Status
Today our seeing monitor delivers a measurement of the Fried parameter every 10s and can work in night time and day-time configuration using bright stars and the Sun as light sources respectively. We have taken it to the Jungfraujoch Observatory for 1st light and since then to the solar telescope in Locarno (IRSOL) to validate day-time measurements. At this point we intend to add more functionalities to the instrument and in particular

| Feature | Status and Timeline |
|---|---|
| Determination of the coherence time $\tau_0$. This will require faster acquisition that our camera can provide. | We have procured an ST-402 camera from SBIG, which we intend to operate in Time Domain Integration mode<br>End of 2006 |
| Determination of the wind vectors by cross-correlating the tip-tilt motions between the different sub-apertures. Note that this requires 3 sub-apertures not collinear in the pupil plane, which is non trivial in our day-time optical set-up | 1st semester of 2007, pending on fast acquisition with TDI |
| Improve observing efficiency. Because of limited pointing precision and the use of a mobile tripod, the guide star is often out of the 3arcmin field of the camera. A multi-port interface with a rotating mirror is foreseen | The interface box has been the object of a student contest and the best design will be selected and built.<br>1st trimester of 2007 |

Conclusion

The seeing monitor is currently producing measurements of the Fried parameter in day-light and night-light. In the next 6 month measurement of coherence time and wind vectors will be added.

We are looking for opportunities to put our instrument to use and are welcoming proposals from observers for measurement campaigns and improvements.